

VISUALIZATION OF LOWER EXTREMITY LYMPHEDEMA IN THE SAME COHORT USING ^{99m}Tc -HUMAN SERUM ALBUMIN AND ^{99m}Tc -PHYTATE LYMPHOSCINTIGRAPHY WITH SPECT-CT

T. Koike, Y. Yabuki, N. Miki, Y. Yamamoto, K. Kokubo,
S. Kitayama, J. Maegawa

Department of Plastic and Reconstructive Surgery (TK,NM), Yokohama City University Medical Center, and Department of Plastic and Reconstructive Surgery (YY,YYa,KK,SK,JM) Yokohama City University Hospital, Yokohama, Kanagawa, Japan

ABSTRACT

Lymphoscintigraphy with single-photon emission computed tomography (SPECT-CT) is useful in diagnosing lymphedema. However, there are multiple timings, techniques, and tracers utilized worldwide without any comparison. We examined and compared the image clarity with two different radiotracers, ^{99m}Tc -human serum albumin (HSA) and ^{99m}Tc -phytate (phytate), in the same patients. The study retrospectively examined 46 limbs of 36 patients who underwent lymphoscintigraphy using HSA and phytate from January 2013 to September 2018. Tracer accumulation in the lymph nodes, linear pattern (LP), and dermal backflow (DBF) were qualitatively analyzed; contrast-to-noise ratios (CNR) of DBF and standardized uptake value ratio (SUVR) of LP were also quantitatively analyzed. Neither lymph node accumulation nor DBF identification showed significant difference. However, a significant difference was observed between the LP identification of the unaffected ($p<0.001$) and affected sides ($p<0.001$). On quantitative evaluation, CNR and SUVR of LP was significantly higher with HSA than with phytate ($p<0.001$). SUVR of LP was also significantly higher with HSA than with phytate in both unaffected ($p=0.002$) and affected ($p=0.005$)

sides. Overall, images acquired with HSA were clearer than that with phytate, and the identification of LP was particularly better with HSA than with phytate. Thus, lymphoscintigraphy using HSA is preferred over phytate for both diagnosis and evaluation of disease severity and surgical site selection.

Keywords: lymphoscintigraphy, single-photon emission computed tomography, SPECT-CT, human serum albumin, phytate

Lower extremity lymphedema is a refractory condition with primary and secondary etiologies, such as infection, trauma, and as complications of malignant pelvic tumor resections. Peripheral lymphatic stasis results from impaired lymphatic flow in the central lymphatic vessels. Consequently, collateral pathways of lymphatic flow can be formed, and edema develops due to lack of lymph flow in the subcutaneous tissues and dermis.

In such cases of lymphedema, proper visualization, diagnosis, and severity assessment of this pathological lymphatic flow is clinically important. Lymphoscintigraphy, near-infrared fluorescent imaging (NIRF), magnetic resonance lymphography, and lymphoscintigraphy with single-photon emission computed tomography (SPECT-CT) are used

to diagnose lymphedema (1). NIRF can visualize the dynamics of lymph flow in real-time and is a useful imaging modality during surgery (2,3). However, tissue penetration of NIRF is limited, with a maximum observable depth of 20 mm. Moreover, an information bias exists because of subjectivity in observation and maintenance of records. In contrast, lymphoscintigraphy is advantageous because it can objectively evaluate tissues deeper than NIRF and is useful for the diagnosis and classification of lymphedema severity (4,5). Recently, more advanced equipment has enabled a clearer visualization of dermal backflow (DBF) and linear patterns (LP) of lymphatic vessels. Lymphoscintigraphy is the worldwide gold-standard method for diagnosis and severity assessment because it provides highly objective imaging findings (1,2,4-9). However, one problem with lymphoscintigraphy is that the imaging conditions, such as radiotracer selection and protocol are not standardized. In particular, multiple radiotracers are being used, and the radiotracer approved in each country is different; therefore, a unified testing strategy is lacking globally. In lymphoscintigraphy, ^{99m}Tc -labeled tracers, such as ^{99m}Tc -sulfur colloid, ^{99m}Tc nanocolloid, ^{99m}Tc -human serum albumin (HSA), ^{99m}Tc -tin colloid, ^{99m}Tc -rhenium colloid, and ^{99m}Tc -phytate (phytate), are all used for imaging. These radiotracers differ in terms of particle size, binding stability, and acquired image features. For example, the larger the particle size of the radiotracer, the higher the possibility of them being trapped in the lymph nodes and the lower the removal or disappearance from the injected site. Reports indicate that the intraoperative identification rate of phytate in the sentinel lymph nodes after breast cancer surgery is better than that of HSA (10). However, it is not clear which radiotracer is best for imaging abnormal lymphatic vessels and DBF with lymphedema. Different radiotracers have been investigated with different patients for imaging lower extremity lymphedema (10,11), but to our knowledge, no study has evaluated and compared different radiotracers in the same patient.

For follow-up of patients with lymph-

edema, we perform not only quantitative evaluation, such as limb circumference, but also qualitative evaluation, such as lymphoscintigraphy to evaluate lymphatic function, repeatedly, on a regular basis. During long-term evaluation, the supply of HSA became unstable due to manufacturing challenges, and we switched to a different radiotracer (phytate). Consequently, we obtained an opportunity to perform lymphoscintigraphy with SPECT-CT on the same patient using two types of radiotracers-HSA and phytate-at different time points. This study aimed to investigate the suitability of radiotracers C HSA and phytate C for objective evaluation and imaging of patients with lower extremity lymphedema.

MATERIALS AND METHODS

Patient Characteristics

From January 2013 to November 2018, 767 patients underwent lower lymphoscintigraphy. Of these, 39 patients underwent lymphoscintigraphy using HSA and phytate. Patients with deep vein thrombosis, chronic heart failure, and generalized edema were excluded. We also excluded three patients and two limbs with worsened International Society of Lymphology stage (1) or Maegawa classification (4) (*Table 1*) in order to evaluate a cohort at the same clinical stage. We enrolled 36 patients (46 limbs) with lower extremity lymphedema and observed no significant changes in symptoms or limb circumference during that time.

The clinical data and Maegawa classification of all patients are listed in *Table 2*.

From the medical chart of the included patients, we examined the interval between tests of lymphoscintigraphy with HSA and phytate, and whether lymphaticovenous anastomosis (LVA) was performed during the study period.

This study was approved by the local ethics committee (B151105012) and was performed in accordance with the ethical guidelines of the Declaration of Helsinki. All subjects provided written informed consent.

TABLE 1
The Maegawa Classification for use In Grading Patients Based on
Their Leg Lymphoscintigraphic Findings

Maegawa Classification	
Type I	Recognition of obvious inguinal lymph nodes and lymphatics along the great saphenous vein, and/or lymph stasis in the collateral lymphatics.
Type II	Dermal backflow can be seen in the thigh.
Type III	No inguinal lymph nodes are detected. Dermal backflow can be seen in the thigh and/or leg.
Type IV	Recognition of dermal backflow and lymph stasis in the leg.
Type V	Dermal backflow can be seen only in the foot.

TABLE 2
Study Patient Characteristics and Maegawa Classification

	Cases (n=36)
Age (year), mean (SD)	57 ± 14
Sex, n (female/male)	33/3
Primary, n	9
Secondary, n	27
Unilateral, n	24
Bilateral, n	12
Maegawa classification	Limbs (n=46)
I	0
II	8
III	11
IV	19
V	8

Lymphoscintigraphy with SPECT-CT Protocol

Lymphoscintigraphy using HSA (FUJIFILM RI Pharma Co. Ltd., Tokyo, Japan) and phytate (FUJIFILM RI Pharma Co. Ltd., Tokyo, Japan) was performed at different time points. Forty MBq of radiotracers in 0.2 ml was injected subcutaneously into the first and fourth web spaces of each foot using a 27-gauge needle to a total of 160 MBq. The injections were administered continuously without any interval. After the injections, patients did not receive any massage or undergo passive exercise load, except for daily activities such as walking and standing. Images were acquired using a SPECT-CT combined system equipped with a dual-head gamma camera

(Symbia T16; Siemens Healthcare Japan, Tokyo, Japan), 120 minutes after the injection. The injection sites were covered with a lead shield.

SPECT-CT images were acquired over a period of 25.2 minutes and a total of 36 views were obtained by both detectors, with 180 degrees of rotation for each camera. All images were acquired with 140 keV photopeak using a 21% symmetrical energy window. The image matrix size was 128 × 128, and a low-energy high-resolution collimator was used.

The data were reconstructed using an iterative method based on an ordered subset expectation maximization algorithm utilizing 10 iterations and 6 subsets with resolution correction. A 13.6-mm Gaussian filter was used for smoothing. The pixel size was 4.8 mm. Both SPECT and CT axial slices were generated using the software application package (Siemens), which was also used for fusing the CT and SPECT images.

Maximum Intensity Projection (MIP) images were generated for visualization, and quantitative evaluation.

Visual Evaluation

We assessed whether the images acquired with each radiotracer could be evaluated properly and also evaluated the radiotracer accumulation at the unaffected sides (n = 24) in patients with unilateral lower extremity lymphedema.

First, we evaluated whether inguinal

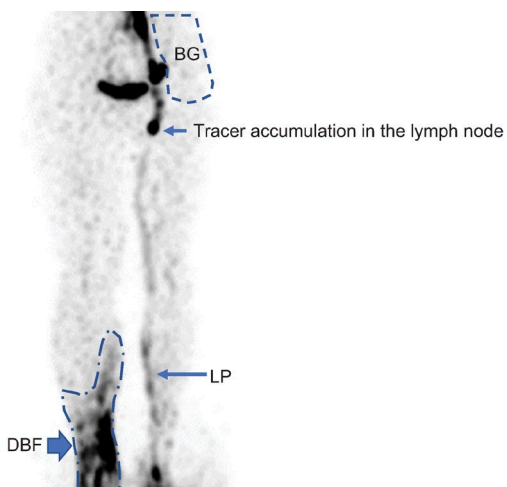


Fig. 1. Maximum intensity projection (MIP) image of a Maegawa classification type 4 right lower leg lymphedema. Background (BG) was set on one flank region. Linear patterns (LP) were seen on the affected and unaffected sides, and dermal backflow (DBF) on the affected side was identified and evaluated.

lymph node accumulation and LP were visualized by HSA and phytate, respectively, at the unaffected sides. Next, we evaluated whether DBF and LP were visualized by HSA and phytate at the affected sides ($n = 46$). Cases were counted as positive if each radiotracer was visualized at one place (*Fig. 1*). All evaluations were performed by two experienced surgeons (T.K. and Y.Y.), while two physicians scored the two parameters. All disagreements were resolved by reaching a consensus.

Quantitative Evaluation

Using the SYNAPSE VINCENT ver 5.3.0001 tool (Fuji film, Tokyo, Japan), we set the region of interest (ROI) for each DBF on lymphoscintigraphy images identified using the two types of radiotracers and measured the average radioactivity.

The background (BG) was set on one flank region without the kidney, ureter, and bladder (*Fig. 1*). The contrast-to-noise ratios (CNR) of each DBF were measured with both HSA and phytate (formula 1):

$$\text{CNR} = [\text{Mean (ROI DBF)} - \text{Mean (ROI BG)}] / [\text{SD (ROI BG)}]$$

(formula 1) where, Mean (ROI DBF) represents the mean ROI of DBF; Mean (ROI BG) indicates the mean background counts; and SD (ROI BG) indicates the standard deviation of background counts.

We evaluated the lymphatic vessels in the images of lower limbs in which LPs were confirmed with both HSA and phytate. The ROI was set for each LP and the standardized uptake value max (SUVmax) of radioactivity was measured. SUV ratio (SUVR) was defined as the ratio of SUVmax and Mean (ROI BG) (formula 2). Measurements were made at both unaffected and affected sides. $\text{SUVR} = [\text{SUV max (LP)}] / [\text{Mean (ROI BG)}]$ (formula 2).

We chose SUVr because the actual diameter of the lymphatic vessel is approximately 1 mm and the ROI setting is not appropriate for estimating CNR.

Statistical Analyses

Radiotracer accumulation in the lymph nodes, LP, and DBF was evaluated by visual examination and the data were analyzed using Fisher's exact test. CNR of DBF and SUVr of LP were evaluated by quantitative examination and the data were analyzed by Wilcoxon signed-rank test. A P-value < 0.05 was considered statistically significant. All statistical analyses were performed with EZR Version 1.37 (12) (Saitama Medical Center, Jichi Medical University, Saitama, Japan), which is a graphical user interface for R (The R Foundation for Statistical Computing, Vienna, Austria). More precisely, it is a modified version of R commander with added statistical functions that are frequently used in biostatistics.

RESULTS

Patient Characteristics

All cases were tested first with HSA followed by phytate. The interval between tests was $1,099 \pm 388$ days. A total of 38/46 (83%) limbs had LVA treatment between lymphoscintigraphy with the two radiotracers.

TABLE 3
Visual Evaluation of Lymphoscintigraphic Image Patterns at the Affected
(n=24) and Unaffected Sites (n=46) (Fisher's exact test)

	HSA	Phytate	P-value
Tracer accumulation in the lymph node (unaffected site; n=24)	24	24	1
LP (unaffected site; n=24)	24	10	<0.001*
LP (affected site; n=46)	40	18	<0.001*
DBF (affected site; n=46)	45	41	0.203

LP, linear pattern; DBF, dermal backflow; *Statistically significant

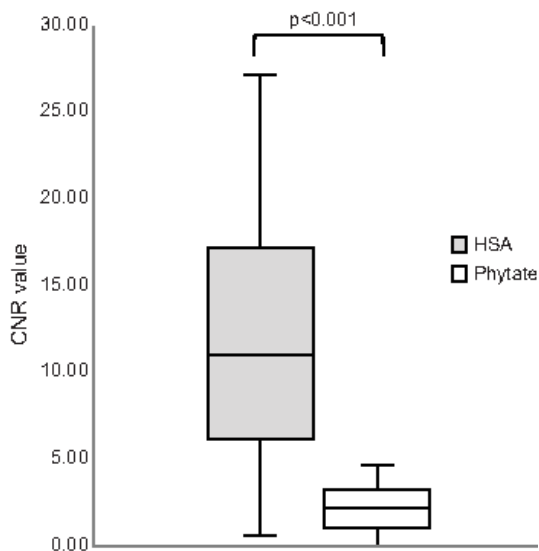


Fig. 2. Comparison of CNR of DBF between HSA and Phytate tracers. (Wilcoxon signed rank test). HSA, ^{99m}Tc -human serum albumin; Phytate, ^{99m}Tc -phytate; DBF, dermal backflow; CNR, contrast-to-noise ratios

Visual Evaluation

On the unaffected side, both HSA and phytate showed lymph node accumulation in all cases. On the unaffected sides, LP was visualized in 24/24 (100%) limbs with HSA and in 10/24 (42%) limbs with phytate (significant difference, $p < 0.001$). Similarly, on the affected sides, LP was visualized in 40/46 (87%)

limbs with HSA and in 18/46 (39%) limbs with phytate (also significant difference, $p < 0.001$). There was no significant difference in the visualization of DBF ($p = 0.203$) (Table 3).

Quantitative Evaluation

In 41 limbs, the background counts were $1,224 \pm 600$ for HSA and $2,315 \pm 1,099$ for phytate. In 41 limbs with DBF, confirmed by HSA and phytate, the CNR with HSA (12.5 ± 8.5) was significantly higher than that with phytate (3.1 ± 3.1) ($p < 0.001$) (Fig. 2). In 10 limbs on the unaffected side, the SUVR of LP was significantly higher with HSA (17.4 ± 24.1) than with phytate (3.3 ± 1.6) ($p = 0.002$). In 18 limbs on the affected side, the SUVR of LP was significantly higher with HSA (13.8 ± 10.3) than with phytate (5.1 ± 3.6) ($p = 0.005$) (Fig. 3).

DISCUSSION

This study investigated the feasibility of using two radiotracers C HSA and phytate C for objective evaluation and imaging of patients with lower extremity lymphedema. Lymphoscintigraphy with SPECT-CT was performed on the same patients using the two radiotracers at different time points. In all patients, lymph nodes were visualized with both HSA and phytate on the unaffected sides. However, phytate was particularly poor in rendering LP, and also conferred a small CNR

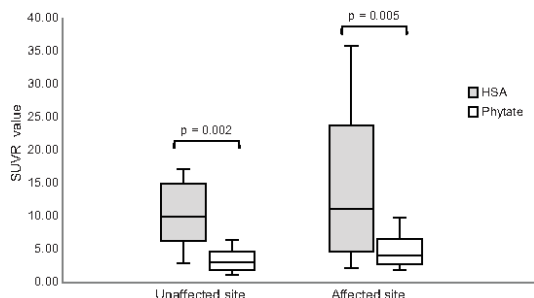


Fig. 3. Comparison of SUVR of the linear pattern SUVR between HSA and Phytate at the unaffected and affected sites (Wilcoxon signed rank test). HSA, ^{99m}Tc -human serum albumin; Phytate, ^{99m}Tc -phytate; SUVR, standardized uptake value ratio

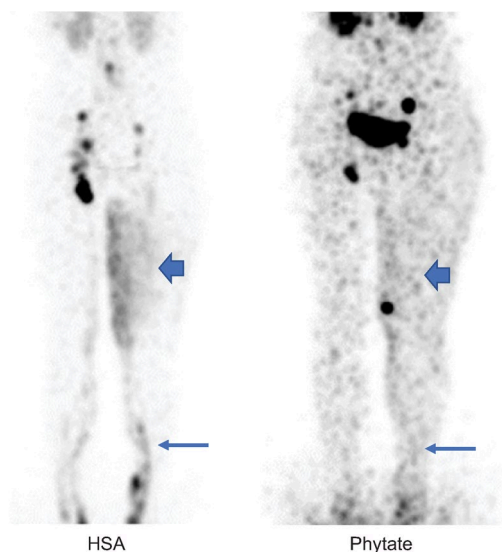


Fig. 4. Maximum intensity projection (MIP) image of HSA and Phytate in the same patient. The thick arrow indicates dermal backflow (DBF), and the thin arrow indicates linear pattern (LP). In the HSA image, both DBF and LP show good visualization. HSA, ^{99m}Tc -human serum albumin; Phytate, ^{99m}Tc -phytate

for DBF. Therefore, HSA rendering was better on both visual examination and quantitative evaluation. The reason why LP and DBF were poorly visualized in phytate was that the background count was high, uneven, and the contrast with the background was low (Fig. 4). In addition, the difference in the images could be

because ^{99m}Tc -phytate binds to Ca^{2+} and form colloid after injection, whereas ^{99m}Tc -HSA remains as such in the lymphatic vessels.

The suitable particle size for lymphoscintigraphy, including sentinel lymph node biopsy and visualization of normal lymphatic vessels, was reported to be 50-70 nm (13), and the radiotracers used were HSA (2-3 nm), tin colloid (400-5,000 nm), sulfur colloid (100-400 nm) and phytate (100-1,000 nm) (14). In addition to particle size, temperature and pH of lymph or the interstitial fluid may affect radiotracer uptake and its transport (14). Also, binding stability of the radiotracer may have an effect. However, unlike sentinel lymph node biopsy and visualization of normal lymphatic vessels, the visualization of lymphedema does not solely depend on the particle size of the radiotracer used. In patients with lymphedema, the lymph vessels are narrowed, obstructed, and their lymph transport capacity is reduced. Therefore, when lymph nodes are present, the lymph nodes on the affected side take longer to demonstrate tracer than that of lymph nodes on the unaffected side (15).

HSA has been widely used in lymphoscintigraphy because it facilitates good visualization of the lymphatic vessels because of its binding stability and rapid absorption under the skin (16-19). There was concern about early washout, but the imaging of LP and DBF were good in this study.

Of the 40 limbs with LP imaged by HSA in this study, 22 (55%) were not imaged by phytate at the affected side. Therefore, the presence of subcutaneous lymphatic vessels and collateral formation cannot be identified on the phytate images. In addition, even on the unaffected sides, HSA conferred a higher SUVR of LP than that with phytate. This suggests that ^{99m}Tc -HSA has high binding stability and is taken up by lymphatic vessels more slowly or flows more slowly than ^{99m}Tc -phytate after diffusing into the extracellular matrix. Therefore, it may be better to visualize DBF with HSA because the time taken by it to leak from the lymphatic vessels is longer. By obtaining an image with high clarity, more detailed localization of DBF and LP existing in DBF, can be identified. Thus, the clinical

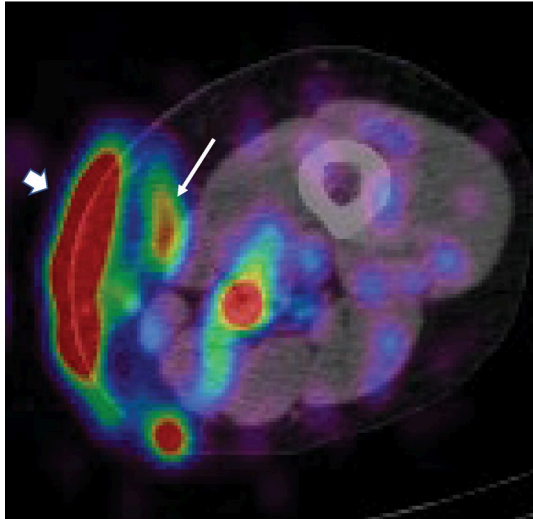


Fig. 5. An axial lymphoscintigraphy image acquired with SPECT-CT. The thick arrow indicates dermal backflow (DBF), and the thin arrow indicates linear pattern (LP). LP can be confirmed on the backside of DBF.

utility is improved not only in terms of severity evaluation but also as a method for identifying lymphatic vessels.

We evaluated lymphoscintigraphy images acquired for 120 minutes. However, there are no uniform protocols and guidelines for the evaluation time of lymphoscintigraphy and evaluation time varies depending on the report. Maclellan et al (20) reported that there was no correlation between lymph nodes and DBF appearance time or limb volume, and lymphoscintigraphy (^{99m}Tc -sulfur colloid) of upper limb lymphedema did not need to exceed 120 minutes. Although there may be a small involvement of lymphovenous shunt (21), our lymphoscintigraphy images taken 120 minutes after HSA injection showed that activity of LP remain higher than the activity of labelled albumin in blood vessels after its dilution in the blood volume. Therefore, we considered that the LP imaged in the lower limb was a significant finding as subcutaneous lymphatic vessels and we believe that the 120-minute evaluate was appropriate. Lymphoscintigraphy is generally used for static evaluation, however, by setting the timing of lymphoscintigraphy imaging multiple times, there

is a possibility of further application of this technique for the evaluation of dynamic lymphatic flow (9). If the lymphatic vessels could be visualized with high-flow velocity, the imaging strategy may also be applicable for the selection of effective LVA.

A limitation of this study is that many cases underwent LVA surgery between the HSA and phytate imaging time points. It is possible that LVA changed the findings of lymphoscintigraphy (22). Although, in theory, LVA should increase lymph flow from the limb and reduce DBF and neither of these were significantly different.

Moreover, in all cases, the phytate scans were performed after the HSA imaging. The progression of lymphedema cannot be ruled out and a bias could be present. However, this study enrolled patients whose Maegawa classification stage did not change. We consider that the bias is small because we compared the same findings in the same patient with the same type and site. Another limitation is that we used the unaffected side as the control. Whether the unaffected side can be used as a control is uncertain. Rossi et al (23) reported that upper limb lymphoscintigraphy showed asymmetric time to reach the axillary lymph nodes in 37.5% of 16 melanoma cases and 50% of 10 normal cases they examined. They were concerned about left-right differences and the effect of physical activity after the injection, which suggested that lymphatic function may also differ between the left and right sides. Our report is useful because the assessment was performed for the same limb of the same patient, rather than on the unaffected side or in comparison to a healthy individual.

Although lymphoscintigraphy has been used as a diagnostic modality for decades, it remains useful in the diagnosis of lymphedema. In addition, improvements in technology and accumulation of evidence have made it possible for lymphoscintigraphy with SPECT-CT to objectively identify lymphatic vessels that are difficult to distinguish by NIRF. Based on these findings, we can identify LP on the back side of DB (Fig. 5), and accordingly perform LVA. SPECT-CT with HSA can visualize deep layers and distinguish deep

lymphatic vessels from deep arteries. This is also made possible by the superiority of HSA over phytate in visualizing LS. Furthermore, we believe that three-dimensional anatomical and kinetic evaluation of the branches connecting the superficial and deep lymphatic vessels is possible in the future, which could confer further usefulness of the imaging technique.

CONCLUSION

Lymphoscintigraphy using HSA and phytate was performed on the same limb of the same patient. Images acquired with HSA were sharper than those acquired with phytate, and especially, had better identification of LP. Lymphoscintigraphy with SPECT-CT using HSA was useful not only for severity assessment but also for lymphatic vessel identification. We expect future development in three-dimensional anatomical evaluation of lymphatic vessels with accuracy.

ACKNOWLEDGMENTS

We thank the staff of the Radiology Department of Yokohama City University Hospital for their advice on image processing.

SOURCES OF SUPPORT

No financial support was received for this study.

CONFLICT OF INTEREST AND DISCLOSURE

The authors declare no competing financial interests exist.

REFERENCES

1. Executive Committee.: The diagnosis and treatment of peripheral lymphedema: 2020 Consensus Document of the International Society of Lymphology. *Lymphology* 53 (2020), 3-19.
2. Kung, TA, MC Champaneria, JH Maki, et al: Current concepts in the surgical management of lymphedema. *Plast. Reconstr. Surg.* 139 (2017), 1003e-1013e.
3. Yamamoto, T, N Yamamoto, Y Fuse, et al: Optimal sites for supermicrosurgical lymphaticovenular anastomosis: An analysis of lymphatic vessel detection rates on 840 surgical fields in lower extremity lymphedema patients. *Plast. Reconstr. Surg.* 142 (2018), 924-930.
4. Maegawa, J, T Mikami, Y Yamamoto, et al: Types of lymphoscintigraphy and indications for lymphaticovenous anastomosis. *Microsurgery* 30 (2010), 437-442.
5. Mikami T., Hosono M., Yabuki Y., et al: Classification of lymphoscintigraphy and relevance to surgical indication for lymphaticovenous anastomosis in upper limb lymphedema. *Lymphology* 2011; 44: 155-67.
6. Weissleder, H, R Weissleder R: Lymphedema evaluation of qualitative and quantitative lymphoscintigraphy in 238 patients. *Radiology* 167 (1988), 729-735.
7. Cambria, RA, P Gloviczki, JM Naessens, et al: Noninvasive evaluation of the lymphatic system with lymphoscintigraphy: A prospective, semiquantitative analysis in 386 extremities. *J. Vasc. Surg.* 18 (1993), 773-782.
8. Mikami, T, A Koyama, K Hashimoto, et al: Pathological changes in the lymphatic system of patients with secondary upper limb lymphoedema. *Sci. Rep.* 9 (2019), 8499.
9. Iimura, T, Y Fukushima, S Kumita, et al: Estimating lymphodynamic conditions and lymphovenous anastomosis efficacy using (99m) Tc-phytate lymphoscintigraphy with SPECT-CT in patients with lower-limb lymphedema. *Plast. Reconstr. Surg. Glob. Open.* 3 (2015), e404.
10. Takei, H, K Suemasu, M Kurosumi, et al: 99mTc-phytate is better than 99mTc-human serum albumin as a radioactive tracer for sentinel lymph node biopsy in breast cancer. *Surg. Today* 36 (2006), 219-224.
11. Svensson, W, DM Glass, D Bradley, et al: Measurement of lymphatic function with technetium-99m-labelled polyclonal immunoglobulin. *Eur. J. Nucl. Med.* 26 (1999), 504-510.
12. Kanda, Y: Investigation of the freely available easy-to-use software 'EZ' for medical statistics. *Bone Marrow Transplant.* 48 (2013), 452-458.
13. Strand, SE, L Bergqvist: Radiolabeled colloids and macromolecules in the lymphatic system. *Crit. Rev. Ther. Drug Carrier Syst.* 6 (1989), 211-238.
14. Szuba, A, WS Shin, HW Strauss, et al: The third circulation: Radionuclide

- lymphoscintigraphy in the evaluation of lymphedema. *J. Nucl. Med.* 44 (2003), 43-57.
15. Toyserkani, NM, S Hvidsten, S Tabatabaeifar, et al: Tc-99m-human serum albumin transit time as a measure of arm breast cancer-related lymphedema. *Plast. Reconstr. Surg. Glob. Open.* 5 (2017), e1362.
 16. Nawaz, K, MM Hamad, S Sadek, et al: Dynamic lymph flow imaging in lymphedema. Normal and abnormal patterns. *Clin. Nucl. Med.* 11 (1986), 653-658.
 17. Ohtake, E, K Matsui: Lymphoscintigraphy in patients with lymphedema: A new approach using intradermal injections of technetium-99m human serum albumin. *Clin. Nucl. Med.* 11 (1986), 474-478.
 18. Glass, EC, R Essner, DL Morton: Kinetics of three lymphoscintigraphic agents in patients with cutaneous melanoma. *J. Nucl. Med.* 39 (1998), 1185-1190.
 19. Samuels, LD: Lymphoscintigraphy. *Lymphology* 20 (1987), 4-9.
 20. Maclellan, RA, D Zurakowski, S Voss, et al: Correlation between lymphedema disease severity and lymphoscintigraphic findings: A clinical-radiologic study. *J. Am. Coll. Surg.* 225 (2017), 366-370.
 21. Stamp, GF, AM Peters: Peripheral lymphovenous communication in lymphoedema. *Nucl. Med. Commun.* 33 (2012), 701-707.
 22. Hara H, M Mihara: Postoperative changes in lymphoscintigraphic findings after lymphaticovenous anastomosis. *Ann. Plast. Surg.* 83 (2019), 548-552.
 23. Rossi, M, R Grassi, R Costa, et al: Evaluation of the upper limb lymphatic system: A prospective lymphoscintigraphic study in melanoma patients and healthy controls. *Plast. Reconstr. Surg.* 138 (2016), 1321-1331.

Tomoyuki Koike, MD
Department of Plastic and Reconstructive Surgery
Yokohama City University Medical Center
4-57, Urafune-cho, Minami-ku
Yokohama, Kanagawa, 232-0024, Japan
Fax: 81-045-231-1846
Tel: 81-045-261-5656
tomo_koi@yokohama-cu.ac.jp